scientific reports

Check for updates

OPEN

Accuracy of the HeartMate 3 Left Ventricular Assist Device Flow Estimation

Theodor Abart[1], Marko Grujic[1], Philipp Aigner[1], Michael Röhrich[2], Stefan Jakubek[3], Daniel Zimpfer[1] & Marcus Granegger[1]✉

Left ventricular assist devices (LVADs), such as the HeartMate 3 (HM3), are a treatment option for advanced heart failure (HF). Non-invasive monitoring of heart-pump interaction is crucial but relies on estimated parameters only. Despite the widespread clinical utilization of HM3 estimated flow rate (Q_{est}) and pulsatility index (PI) their accuracy was not yet quantified. This study assessed the HM3 monitoring by describing underlying physical characteristics, estimation algorithms and deriving accuracy of estimates in clinical practice. Identification measurements were performed to quantify the physical characteristics and mechanisms of flow estimation. Virtual patients coupled to a hybrid hock circulatory loop were employed to evaluate estimator accuracies in realistic operating conditions. The correlation between Q_{est} and torque-generating-current was strong ($r^2 > 0.99$, $p < 0.001$), confirming that estimation is based on speed, current, and viscosity. Also, the PI is directly derived from current. However, the underlying current/flow relationship is ambiguous (one current value corresponds to two flow rates). The HM3 flow estimator showed an RMSE of 1.63 L/min and a correlation coefficient of $r = 0.86$ ($p < 0.001$). The non-linear relationship obscures the systolic portion of flow as current declines during peak systole at higher flow rates. HM3 monitoring is unable to accurately represent the actual hemodynamics, particularly in the transition between full support and partial support, which is a region highly prevalent and crucial in clinical practice. It is therefore recommended to interpret values and trends of the HM3 monitoring system with caution.

Abbreviations

AoP	Aortic pressure
AV	Aortic valve
BTT	Bridge to transplantation
DT	Destination therapy
HF	Heart failure
HM3	HeartMate 3
HMCL	Hybrid mock circulatory loop
HTx	Heart transplantation
ID	Inner diameter
IT	Torque-generating-current
LV	Left ventricle
LVAD	Left ventricular assist device
LVP	Left ventricular pressure
MCL	Mock circulatory loop
PI	Pulsatility Index
Qest	Estimated pump flow
Qmeas	Measured flow rate
RMSE	Root mean square error
μ	Viscosity
ω	Rotational speed

[1]Christian Doppler Laboratory for Mechanical Circulatory Support, Department of Cardiac and Thoracic Aortic Surgery, Medical University of Vienna, Vienna, Austria. [2]Department of Anesthesia, Intensive Care Medicine and Pain Medicine, Medical University of Vienna, Vienna, Austria. [3]Division of Control and Process Automation, Institute of Mechanics and Mechatronics, Vienna University of Technology, Vienna, Austria. ✉email: marcus.granegger@meduniwien.ac.at

Left ventricular assist devices (LVADs) are an established and advancing complement to the gold standard heart transplantation (HTx) for patients with medically-refractory end-stage heart failure (HF) with reduced ejection fraction[1]. Third-generation magnetically levitated centrifugal-flow LVADs, such as the HeartMate 3 (HM3) (Abbott, North Chicago, Illinois, USA) are implanted apically into the left ventricle (LV) to support the weakened heart by bypassing either part of (partial support) or the total cardiac output (full support) to the ascending aorta[2,3].

With over 60% of patients being supported in partial support and the pump ejecting in parallel to the native heart[4,5], accurate hemodynamic monitoring is essential for patient management—namely, to assess cardiac function and optimize heart-pump interaction. Further, monitoring is a prerequisite for future work on adaptive LVAD support settings that could restore circulatory function or promote cardiac recovery. However, monitoring capabilities in current LVADs are limited with hemodynamic sensors for measuring pump flow or LV pressure (LVP) not implemented as they would increase system complexity, costs, fault potential and add the need for recalibration[6,7]. To overcome this challenge, continuous, non-invasive real-time diagnostics of hemodynamic parameters based on readily available technical LVAD pump parameters would be favorable and essential for determining the cardiovascular status such as cardiac functions (contractility and relaxation)[8,9], AV opening[10–13], heart rate variability[14], and suction[15]. Reliable measurement and/or estimation of flow rate and pump head pressure together with blood viscosity would permit the application of already published and previously mentioned diagnostic algorithms to any present or future LVAD and therefore pave the way towards physiological control and optimization of cardiac mechano-energetics.

State-of-the-art LVADs, including the HM3, estimate an average flow rate based on the pump/motor-characteristics, which are readily available[16]. The HM3 provides the user with an average flow value together with the pulsatility index" (PI), which is supposed to describe the flow rate amplitude.

These HM3 pump parameters are increasingly utilized as clinical markers[16–18] and in research[19–21]. However, as previously schematically described by Belkin et al., flow estimation of the HM3 is challenged by a non-monotonic current-flow relationship[16]. However, implications of this relationship on the accuracy and potential for advanced monitoring capabilities of the HM3 monitoring system (flow estimation and pulsatility index) have not yet been investigated in a systematic manner.

The aim of this study was to quantify the accuracy of the clinical HM3 monitor, namely estimated flow rate and PI, by addressing the underlying physical characteristics of the HM3 pump-motor assembly. Based on these analyses, we characterize and numerically describe the behavior of monitoring parameters in clinical settings and assess their potential for hemodynamic diagnostics.

Methods

In a first step, to describe the flow estimation mechanism, the relationships of intrinsic pump signals were compared to the measured flow rate signal over the entire operating range at different viscosities for static operating points. Next, to analyze accuracy of flow estimation in the LVAD patient cohort, realistic hemodynamic signals were generated in a hybrid mock circulatory loop (HMCL) and estimated flow rates and PI values were compared to measured ones.

Test bench setup

The HMCL previously established by Bender et al.[22], was employed with the HM3 integrated by connecting the pump inflow to the ventricular reservoir and the outflow to the aortic reservoir using tubing matching the HM3 outflow graft characteristics (Inner Diameter (ID) = 14 mm, length = 200 mm). The Hardware-in-the-Loop setup (Fig. 1) combines a hydraulic system with a pneumatic system to apply various conditions to the inflow and outflow of the pump and a gear pump to control the fluid levels of the two reservoirs. Aqueous glycerol solutions with varying mixture ratios were used as blood-mimicking fluids. A lumped parameter model of the cardiovascular system was used to simulate a virtual patient, calculate the pressure conditions for LVP and aortic pressure (AoP) at each timestep and feedback the measured flow rate for the calculation of the cardiovascular status at the next timestep at a sampling rate of 1 kHz. The real-time interface was realized using the dSpace MicroLabBox (dSpace GmbH, Paderborn, Germany) platform together with dSpace Control Desk (v. 2023-A, dSpace GmbH, Paderborn, Germany).

The numerical lumped parameter cardiovascular model was implemented as an open loop model with a time-varying elastance and a nonlinear end-systolic and end-diastolic pressure volume relationship according to Colacino et al.[23], and Bender et al.[22], using the Simulink environment (Simulink 2023-A, MathWorks, Inc., Natick, MA, USA). The model parameters were adapted to match the hemodynamics described by Gupta et al.[24], and then adapted to achieve a typical full-support AV closed, low pump flow pulsatility) and a partial support (AV open, high pump flow pulsatility) condition.

Pressures were measured at the LV reservoir, directly after the pump and at the aortic reservoir (TruWave, Edwards Lifesciences Corp., Irvine, CA, USA) and flow rate (Sonoflow CO55, Sonotec GmbH, Halle, Germany) was measured directly after the pump at the outflow tubing. Temperature and viscosity (devil, AveniSense, Wika Group, Klingenberg am Main, Germany) were measured at the backflow from the aortic to the LV reservoir, where also the heat exchanger (CSC 14 Cardioplegia Heat Exchanger, LivaNova PLC, London, Great Britain) and the gear pump (UP2 24 V, Marco, Brecia, Italy) were placed.

The LVAD pump controller was replaced by an RS232 serial communication interface (MAX232, Texas Instruments Inc., USA) connected to the MicroLabBox digital input port, requests for pump data previously observed in the communication protocol were sent to the HM3 and responses containing the current pump parameters were recorded. Pump speed and the hematocrit corresponding to the desired viscosity were set prior

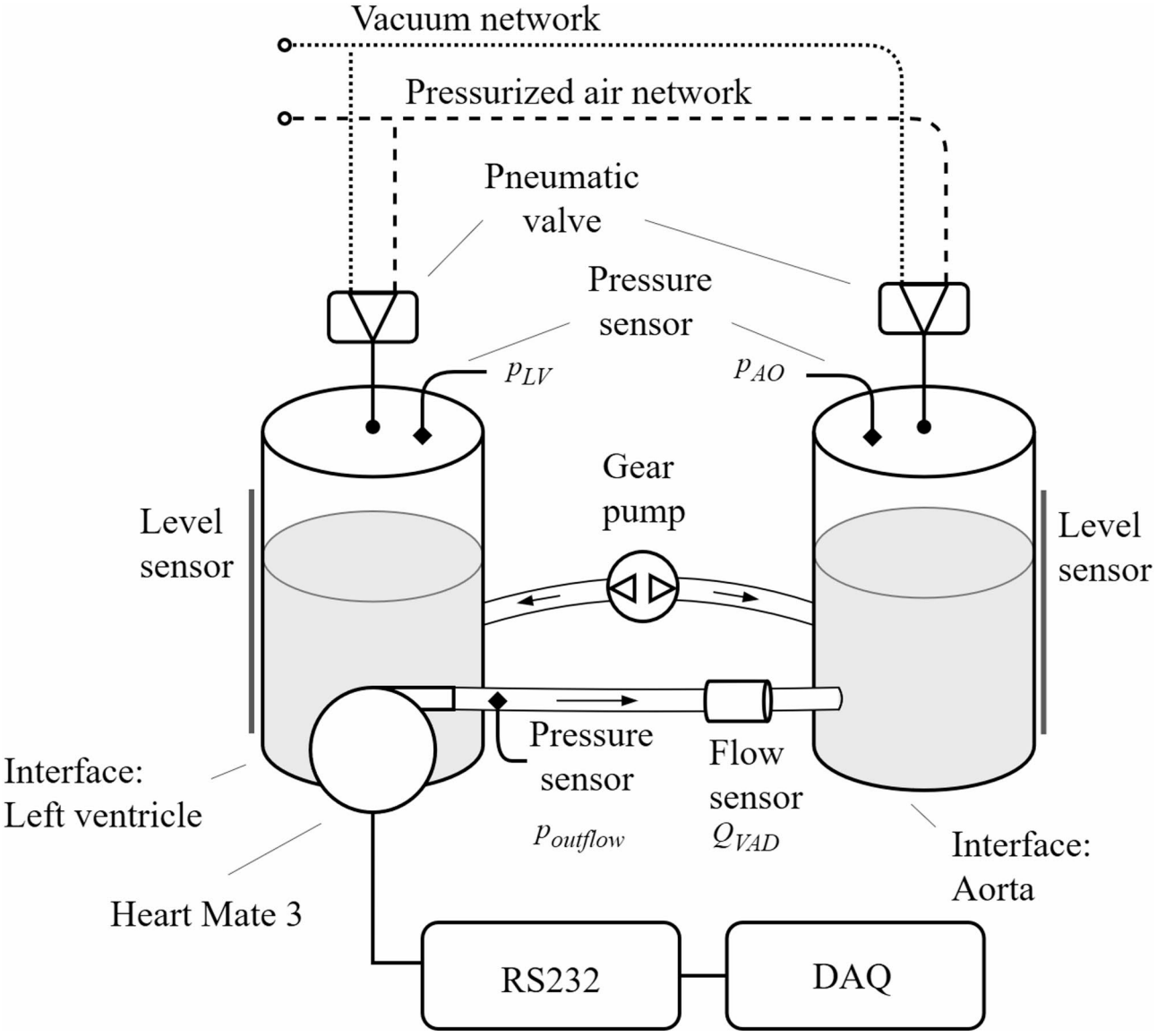

Fig. 1. Hybrid Mock Circulatory Loop (HMCL) used for the measurement process. The hydraulic system is subjected to physiological pressures by using a control algorithm that adjusts the pneumatic proportional valves switching between vacuum network and pressurized network to achieve the desired pressure. The gear pump is used to balance the fluid level of left ventricular (LV) reservoir (left) and aortic (AO) reservoir (right). The HeartMate 3 inflow is introduced to the LV reservoir with its outflow connected to the AO reservoir. An RS232 based pump controller and a data acquisition system (DAQ) for pump parameters are in place. Modified after Bender et al.[22].

to each experiment and the artificial pulse disabled. Each second 30 requests for data were sent to the HM3, resulting in a sampling rate of 30 Hz for pump parameters.

Measurement process

All measurements were performed at three fluid viscosities (μ = 2.5 mPa·, μ = 3.5 mPa·s and μ = 4.5 mPa·s) corresponding to a hematocrit of 22%, 34% and 43%[25,26]. For each viscosity, static, dynamic, and pulsatile identification was performed. Static identification was performed for 5 constant HM3 rotational speeds (ω = 3 krpm, ω = 4 krpm, ω = 5 krpm, ω = 6 krpm, ω = 7 krpm). While the HM3 LVAD speed was set to a constant value, actual flow was measured using the flow probe and the driving current of the gear pump in the backflow path controlled to reach the desired target flow rate value. The target flow rate was incrementally adjusted in 1 L/min steps every 30 s in a stepwise manner from − 1 L/min to the point at which zero head pressure was attained at the given constant HM3 rotational speed. This procedure was repeated for all five HM3 speeds, with data from seconds 15 to 25 of each step sampled as a steady state and processed. Each experiment was repeated 3 times. The dynamic identification was performed by applying sine sweeps of head pressure: the pressure in the aortic reservoir was controlled to a constant value while the pressure in the LV reservoir was applied in the form

of sine sweeps from 0.5 to 14 Hz. The pressure difference was selected to produce flow rates across the whole range of operation (zero flow to zero head pressure) for each speed step. Pump and measurement data with a frequency content from 0 Hz to 4 Hz was considered for further analysis regarding the flow estimation, higher frequency content was not analyzed within the scope of this study. Physiological hemodynamics derived from clinical data[24,27], were acquired for patients with full support (low cardiac contractility, no AV-opening, low flow pulsatility) and partial support (high cardiac contractility, AV-opening, high flow pulsatility) supported each by two pump speeds (ω = 4800 rpm and ω = 5400 rpm). This selection covers typical LVAD patient hemodynamics as well as extreme conditions (pediatric, recovery) to allow for an understanding of the mechanisms of flow estimation across the entire clinically relevant range.

Statistical analysis

For a mechanistic understanding of the flow estimation algorithm in the HM3, relationships between technical pump parameters and Q_{est} were investigated by calculating Pearson correlation coefficients with the aim of identifying the parameter that is correlating the best ($r^2 \approx 1$) with estimated flow.

Root-mean-squared-error (RMSE) was calculated for the difference between Q_{est} and Q_{meas} for the static measurements across the entire operating range. The correlation of Q_{est} and Q_{meas} was described by Pearson correlation for static measurements. Bland-Altman plots were used to assess the agreement between Q_{est} and measured Q_{meas} values by plotting their difference against their mean. This allowed us to evaluate the bias and potential regional dependencies in the differences[28].

The parameter that had been identified as the most relevant for flow estimation was used to calculate a surrogate for the pulsatility index by dividing the difference between the beat-wise maxima and minima by the beat-wise mean.

$$PI = \frac{\max - min}{mean} \tag{1}$$

Correlating this to the estimated pulsatility index of the HM3 by Pearson correlation may reveal whether the pulsatility index is calculated on the same parameter as the flow rate is estimated on. The behavior of the pulsatility index under realistic operating conditions was then investigated by comparing the estimated (technical pump parameter based) PI to the PI based on flow measurements,

the gold standard for PI was defined as:

$$PI_{measured} = \frac{Q_{\text{meas max}} - Q_{meas\ min}}{Q_{meas\ mean}} \tag{2}$$

With the maximal ($Q_{\text{meas max}}$) and minimal ($Q_{meas\ min}$) values representing the beat wise maxima and minima of Q_{meas}. To translate the $PI_{measured}$ to the PI displayed on the HM3, a linear regression model with the following structure was used was used and k and d fitted to translate the measured PI to the 〚PI〛_HM3 in regions of a linear torque-generating current – flow relationship:

$$PI_{HM3} = k * PI_{Measured} + d \tag{3}$$

Results

Working principle of the flow estimator and underlying motor characteristics

In static identification measurements Q_{est} showed a linear relationship with I_T (torque-generating-current, $r^2 = 0.99$, $p < 0.001$) at each μ and ω, indicating that pump flow estimation is solely based on ω, I_T and μ (Fig. 2).

However, the underlying relationship between I_T and Q_{meas} revealed non-linear behavior with non-monotonic, ambiguous behavior at higher flow values (Fig. 3). High Q_{meas} values therefore are accompanied by a decrease in I_T, indicating that Q_{meas} is not an injective function of I_T. An increase of flow is accompanied by an increase in I_T only until the global maxima of I_T values are reached, an increase in flow rate above these points (Fig. 3, blue lines) resulted in lower I_T values (Figure S1).

Accuracy of the flow estimator

Regression analysis (Fig. 4 left) showed a correlation of Q_{meas} and Q_{est} with $r = 0.86$ ($p < 0.001$) over all datapoints ($n = 138$) with a regression slope of 0.75 (an increase in measured flow of 1 L/min increased estimated flow by 0.75 L/min on average). Stratified by speed and viscosity the worst correlation was $r = 0.87$ ($p < 0.001$) at ω = 6000 rpm and the best was $r = 0.94$ ($p < 0.01$) at ω = 3000 rpm, at a viscosity of μ = 3.5 mPa·s and μ = 4.5 mPa·s, respectively.

Bland Altman analysis showed a bias of 0.5 L/min and a better agreement of Q_{meas} and Q_{est} in flow regions around the main operating point of the pump (5.4 L/min, 60 mmHg) but an overestimation in lower regions and an underestimation in higher flow regions was observed (Fig. 4 right). The RMSE between Q_{meas} and Q_{est} was 1.63 L/min (Table S1). RMSE values increased with increasing speed with RMSE = 0.92 L/min at ω = 3000 rpm (lowest investigated speed) and RMSE = 2.04 L/min at ω = 7000 rpm (highest investigated speed). The effect of different viscosities is shown by an overall RMSE of 1.39 L/min at μ = 2.5 mPa·s (lowest investigated viscosity) and of 1.59 L/min at μ = 4.5 mPa·s (highest investigated viscosity). For the main clinical operating range between 4000 rpm and 6000 rpm, the RMSE was 1.54 L/min.

With the static deviations being hard to translate to a dynamic setting such as present in the LVAD under realistic operating, the following will present the results of dynamic sine sweeps that complement the static curves to prove that the static behavior is reflected also in dynamic signals: The dynamic behavior of I_T showed

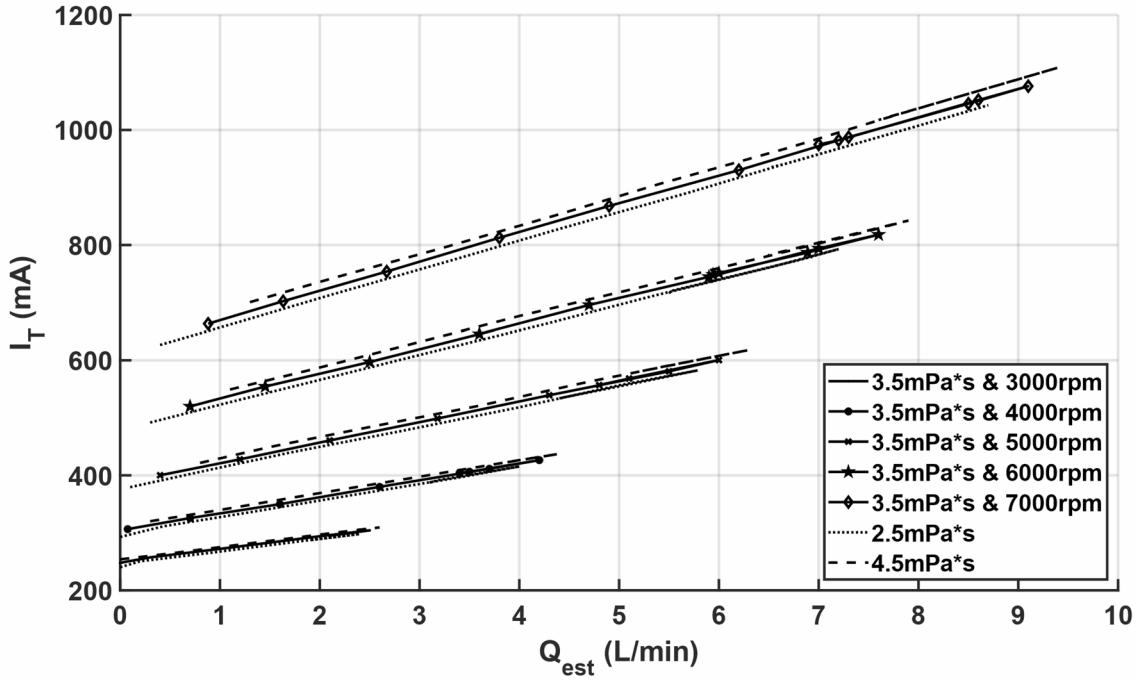

Fig. 2. Estimated flow and torque-generating-current (I_T) for 5 speeds and 3 viscosities applied to the HeartMate 3 (HM3) in static environment. For each setting of ω and μ the correlation of I_T and Q_{est} was linear with r2 = 0.99 and $p < 0.001$.

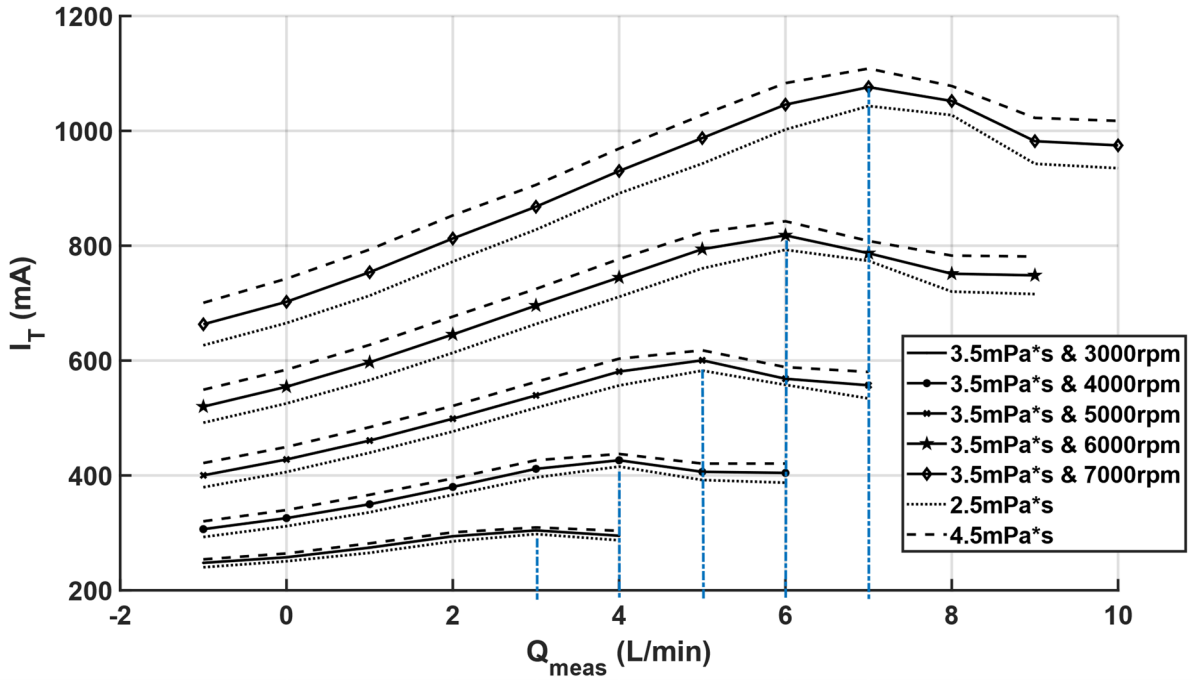

Fig. 3. HeartMate 3 (HM3) static relationship between torque-generating-current (I_T) and measured flow (Qmeas) at three different viscosities and five different speeds in a static environment. The blue lines mark the global maxima of I_T values, reached at 3 L/min, 4 L/min, 5 L/min, 6 L/min, and 7 L/min for a HM3 pump speed of 3 krpm, 4 krpm, 5 krpm, 6 krpm and 7 krpm. An increase in Qmeas above these maxima results in lower IT values.

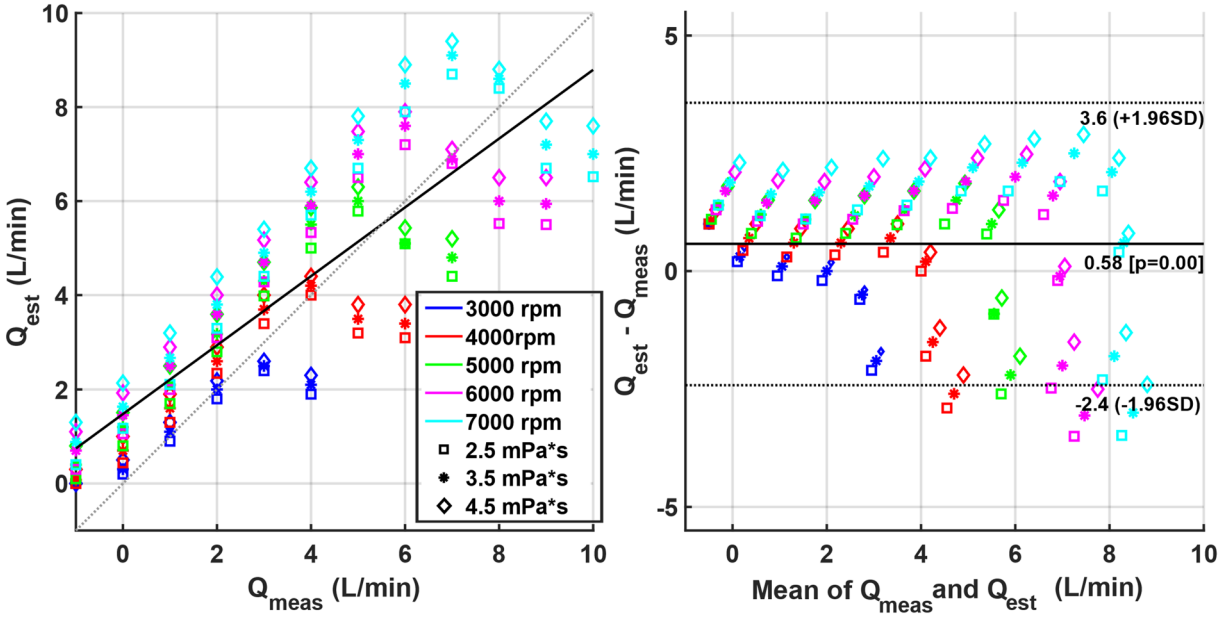

Fig. 4. Accuracy of the HeartMate 3 (HM3) flow estimator calculated based on the static identification measurements. Left: Scatter plot of measured flow (Q_{meas}) versus estimated flow (Q_{est}). Right: Bland-Altman plot showing the agreement between measurement and estimation by plotting the differences between Q_{meas} and Q_{est} (y-axis) over the means of both signals (x-axis).

(Fig. 5) that the instantaneous torque follows the static characteristics and had decreasing values for peak flows that are beyond the I_T maxima. *E*stimated flow in the HM3 is calculated based on the 2-second average of I_T[19] and therefore cannot represent the systolic proportion adequately. RMSE for sine sweep signals was 0.84 L/min (defined as the deviation between Q_{est} and the 15 s moving mean of Q_{meas}), detailed results for all speeds and viscosities are provided (Table S1).

Pulsatility index calculation

The Pulsatility Index (PI) revealed strong correlation with the calculation of PI based on the measured I_T values (3) ($r^2 = 0.99$, $p < 0.001$) suggesting that PI is calculated based on I_T. (Figure S1)

$$PI_{Torque\ Based} = \frac{I_{T\,\max} - I_{T\,min}}{I_{T\,mean}} \tag{4}$$

To translate the PI displayed on the HM3 to the actual PI of the measured pump flow waveform (Eq. 2), a regression model was calculated based on measurements where the HM3 operates in regions of linear I_T - flow behavior and the whole amplitude of the flow pulsatility is reflected in I_T. For simulated patients in partial support and the static reference (displayed PI_{HM3} at static flow) the following regression achieved an r^2 of 0.99:

$$PI_{HM3} = 5.83 * PI_{Measured} + 0.44 \tag{5}$$

Flow estimation and PI under realistic operating conditions

In typical full support hemodynamics with measured flow pulsatilities of 2.36 L/min and 1.52 L/min and a measured mean flow of 2.63 L/min and 4.46 L/min at 4800 rpm and 5400 rpm, the flow was overestimated by 1.41 ± 0.44 L/min (41%).In partial support conditions with higher pulsatility (5.42 L/min and 4.96 L/min) flow was overestimated by 0.65 ± 0.41 L/min (18%) on average.

The percentage error and RMSE values (Table 2) indicate that the estimator performs overall worse in full support compared to partial support. With different rotational speed and viscosity contribution less to the error size (Table 1).

Using the regression described (see Pulsatility Index calculation), a PI was calculated that represents the true flow amplitude based on Q_{meas} and is compared to the PI displayed on the HM3 system controller for all realistic operating conditions and at a viscosity of 3.5 mPa·s: While during full support the PI_{HM3} matches with the PI derived from Q_{meas}, during partial support PI_{HM3} underestimates the true pulsatility by a value of 3.6 or 32% at ω = 4800 rpm and by 2.4 or 33% at ω = 5400 (Table 2).

As visible (Fig. 6) in full support, I_T increases steadily with flow, however in partial support, the maximal I_T value is reached prior to the maximum of the systolic flow, the residual proportion of the flow corresponds to I_T values lower than the maximum and therefore is not contributing to the calculation of PI.

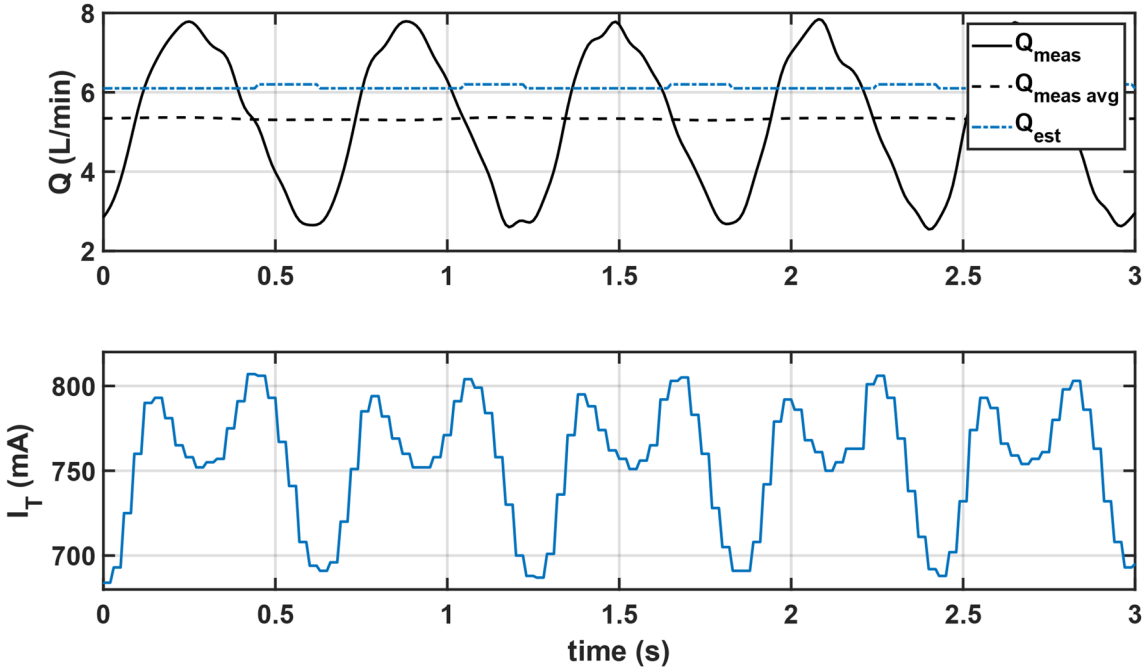

Fig. 5. Behavior of flow (estimated (Q_{est}) and measured (Q_{meas})), torque-generating-current (I_T) and speed during dynamic identification with a sine shaped flow at 96 bpm–1.6 Hz*:* At a flow rate of around 6 L/min and I_T values around 818 mA, I_T decreases regardless of the continuing increase in Q_{meas}. Despite the I_T signal not reflecting the peak flows, Q_{est} overestimates Q_{meas} by 0.83 L/min, this can be explained by the fact that most of the flowrange at 6000 rpm is overestimated as visible in the static characteristics.

	Speeds	2.5 mPa·s	3.5 mPa·s	4.5 mPa·s
Full support	4800 rpm	0.79 L/min (30%)	1.2 L/min (46%)	1.56 L/min (60%)
	5400 rpm	1.19 L/min (26%)	1.66 L/min (37%)	2.05 L/min (47%)
Partial support	4800 rpm	0.15 L/min (5%)	0.57 L/min (19%)	0.97 L/min (33%)
	5400 rpm	0.25 L/min (6%)	0.73 L/min (17%)	1.22 L/min (29%)

Table 1. Absolute and relative errors of heartmate 3 (HM3) flow Estimation at a full and a partial support) for two different rotational speeds and for the three investigated viscosities.

The proportion of the systolic flow that is not reflected by an increasing I_T (Fig. 6 right) was quantified by calculating the highest flows that can theoretically be estimated (Table S2) and comparing them to $Q_{meas\ max}$: At ω = 4800 rpm Q_{meas} systolic flow values were up to 6.22 L/min for partial support and up to 4.05 L/min for full support, at ω = 5400 rpm systolic Q_{meas} were 7.29 L/min and 4.90 L/min respectively for the two conditions. However theoretical estimation maxima given by the I_T maxima were 4.90 L/min at ω = 4800 rpm and 5.50 L/min at ω = 5400 rpm. This led to an offset between maximal Q_{est} and maximal Q_{meas} of 1,32 lpm for ω = 4800 rpm and 1,79 lpm for ω = 5400 rpm (Table S2).

Discussion

In this study we evaluated the HM3 flow estimation, its underlying physical characteristics and their potential for advanced monitoring of cardiovascular function. For this purpose, the underlying mechanisms of flow estimation and PI calculation were described based on static and dynamic measurements. Further, the accuracy of flow rate and PI estimation was assessed under realistic hemodynamic conditions in a HMCL.

We confirmed that the HM3 estimates pump flow solely based on I_T, pump speed and viscosity (user input). The relationship between I_T and Q_{meas} is, however, ambiguous, making it impossible to derive one flow value from a given I_T value, in certain regions. The relationship reaches a maximum at the points displayed in Fig. 3, beyond these maxima, the HM3's estimated flow no longer adheres to this relationship, leading to inaccurate estimations. This is in line with Belkin et al., who already mentioned the static behavior of I_T (without effects of viscosity), however the resulting deviation in flow estimation or PI has not been quantified, and dynamic behavior or realistic operating conditions have not been investigated. Our results revealed that despite an overall correlation between measured and estimated flow with $r = 0.86$, the HM3 flow estimator used in clinical routine

	Partial support – high pulsat.		Full support – low pulsat.	
	PI_{HM3}	Q_{meas} based PI	PI_{HM3}	Q_{meas} based PI
4800 rpm	7.5	11.1	5.6	5.6
5400 RPM	4.8	7.2	2.6	2.4

Table 2. Comparison of torque-generating-current (I_T) derived pulsatility index (PI) values shown on the heartmate 3 (HM3) system controller (PI_{HM3}) and pulsatility index values derived from the measurements of flow pulsatility and converted to the same scale by using a regression model. Partial and full support and two different rotational speeds are compared for a viscosity of 3.5 mPa·s: the pulsatility index values match well during full support, however during partial support the HM3 does not adequately represent pump flow pulsatility, the values calculated directly from the measured flow pulsatility are higher than the values estimated by the HM3.

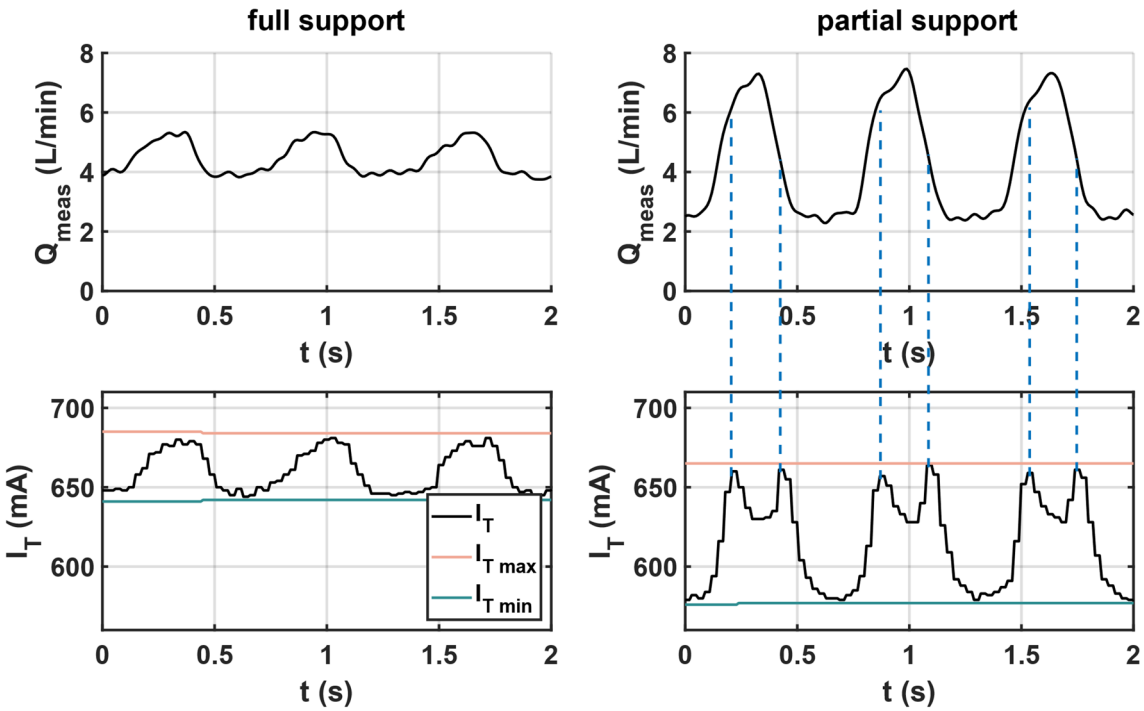

Fig. 6. Measured pump flow (Qmeas) and the torque-generating-current (IT) are shown during cardiac cycles at ω = 5400 rpm and μ = 3.5 mPa·s for full support (left side) and partial support (right side). In the lower right graph, the decrease of IT regardless of the increasing Qmeas is visible. The dashed lines mark the infliction point of IT at this ω (~ 820 mA).

overestimates the flow values in low flow regions and underestimates values in higher flow regions leading to a RMSE of 1.63 L/min in static conditions.

The HM3 uses a well-established method for estimating pump flow in a rotary blood pump, however, the estimation was more accurate for other pumps that were routinely used in clinical routine and that used a similar approach: For the HVAD (Medtronic Inc., Minneapolis, MN) in static operating conditions using aqueous glycerol mixtures the correlation coefficient between measured and estimated flow was > 0.94 and absolute errors were < 1 L/min for all tested states (4 hematocrits and 5 operating points at 11 different speed steps)[29]. Another study could repeat these findings in a dynamic setting and describes an r^2 of 0.96 for in-vitro measured estimated and measured flow in an MCL[30]. The HeartMate II (HM II) estimated flow acquired in 20 patients intraoperatively and compared to ultrasonic flow probe measurement showed an r^2 of 0.56 with an RMSE of 0.8 L/min and a difference of 15–20% for a range of 4 to 6 L/min[16]. However, Belkin et al. described the current in the HM II having an ambiguous relationship at lower flow values, while in the HM3 an ambiguous relationship is present in the higher flow regions[16].

In the HM3 only the mean flow rate without any waveform is made available to the clinicians (Q_{est}), therefore, estimation errors may be partly compensated for during the cardiac cycle by overestimating the diastolic and underestimating the systolic flow. However, when the actual pump flow (Q_{meas}) is aligned asymmetrically between regions of over- and underestimation, an error emerges between Q_{meas} and Q_{est}, which might be the

case in patients with lower flow rates (e.g. smaller or pediatric patients) or patients with a higher contractility and/or lower speed setting.

Further, we showed that the PI used by the HM3 to describe pump flow is solely based on I_T values. In partial support, and therefore in the majority of LVAD patients[4,5], I_T values lie within the nonlinear region of the flow/I_T relationship, where I_T plotted versus Q_{meas} exhibits a local maximum (Fig. 3), therefore I_T values are capped and cannot depict the systolic proportions of the estimated flow, leading to an inadequate representation of pump flow pulsatility by the PI. (Fig. 6).

The presented results have important clinical implications regarding the monitoring of HM3 patients. The non-monotonic behavior of the I_T characteristics leads to erratic results not only in absolute values but also in trends of mean flow rate and PI. For example, a patient supported in full support may initially operate in the linear I_T - Q_{meas} characteristics, where Q_{est} and PI_{HM3} directly reflect changes in flow/pressure head and therefore also residual cardiac function. In the case of e.g. improvement of cardiac function, regions above the maximum I_T will be reached, however, not reflected in Q_{est} and PI_{HM3}. Vice versa also deterioration of cardiac function may not be visible in Q_{est} and PI_{HM3} in a patient with AV opening. Similarly changes in pre- and afterload cannot be reflected in Q_{est} and PI_{HM3} over the entire flow range. Therefore, these parameters should be interpreted with caution and clinical decisions should not be based on theHM3 monitoring system.

Even though not implemented in the current HM3 monitoring, it was previously shown that accurate flow estimation with high frequency bandwidth based on available pump signals bears the potential to accurately determine hemodynamic parameters and cardiac function in patients with a rotary blood pump[31]. Several alternative methods have been described to estimate flow rate or pressure head and viscosity based on pump speed, power consumption/motor current and/or impeller displacement[32–35]. Pumps employing other techniques for determining pump flow were the Incor (Berlin Heart AG, Germany), which used the axial displacement of the magnetically levitated rotor[36,37] or the HeartAssist 5 and aVAD (ReliantHeart Inc., Houston, TX, USA) which had an ultrasonic flow probe integrated[38]. Our work suggests that similar methods should be employed to improve the clinical monitoring of the HM3. This could provide a more accurate estimate in regions where the IT value is ambiguous in relation to flow. Such an approach would, however, require more advanced techniques.

Limitations

Water-Glycerin solutions were used as blood-mimicking fluids as they are ideally suited for simulating the rheological properties of blood and therefore are widely used in cardiovascular MCLs. The dynamic viscosity (μ) was matched with the viscosity of blood at desired hematocrits, however, the density of Glycerol–water is higher than the density of the viscosity matched blood (blood at Hematocrit of 40%: 1062 kg/m3, viscosity matched glycerol-water: 1110 (+ 4.5%))[39]. Therefore, measurements with whole blood could slightly shift the presented results to a quantitative level but basic characteristics will be retained.

As the intrinsic filter and signal processing algorithms are not known, this could lead to slight phase deviations between the measured data and those acquired via the pump electronics data.

Due to the highly heterogeneous patient-specific hemodynamics of LVAD patients, it is challenging to derive a simple statement on how to integrate this knowledge into clinical decision making as the inaccuracy of the flow estimation may change quantitatively and qualitatively with the patient status. Nevertheless, it is inevitable that in a patient with partial support, the systolic flow is reflected incorrectly in the parameter estimation. Changes in systolic flow do not lead to the expected changes in the estimated parameters, which can lead to an inaccurate assessment of cardiac function.

Conclusion

In the HM3 the flow and PI estimation principle is based on the I_T – flow relationship, which is ambiguous in certain flow regimes. This hinders correct estimation of high flow values, which regularly occur during the cardiac cycle in the majority of LVAD patients. The current HM3 flow estimator provides a good approximation of mean flow values at around 4 L/min but will lead to estimation errors and might conceal changes in hemodynamics in most cases due to the highly heterogeneous patient population. The PI inadequately represents flow pulsatility, as the amplitude of underlying IT values does not reflect an increase in systolic flow, particularly in patients on partial support—a condition linked to better outcomes[40] and present in 64% of LVAD patients[5].

Deriving the patient's hemodynamic status from pump parameters and developments towards physiological control, recovery detection, or fault detection rely on accurate parameter estimation, especially of the systolic part of the pump flow waveform and therefore the systolic function of the myocardium. The currently predominant LVAD has technical limitations concerning these crucial aspects as estimated flow shows considerable estimation errors and PI cannot represent flow pulsatility.

Data availability

The data supporting the results of this manuscript are presented in the figures in the results section. Should raw data or other formats be required, the authors are available to provide them upon request. To access the data please contact the corresponding author (Marcus Granegger).

Received: 5 January 2025; Accepted: 22 May 2025
Published online: 30 May 2025

References

1. Jorde, U. P. et al. Jan., The Society of Thoracic Surgeons Intermacs 2023 Annual Report: Focus on Magnetically Levitated Devices, *Ann. Thorac. Surg.*, vol. 117, no. 1, pp. 33–44, (2024). https://doi.org/10.1016/j.athoracsur.2023.11.004

2. Bourque, K. et al. Design rationale and preclinical evaluation of the heartmate 3 left ventricular assist system for hemocompatibility. *ASAIO J.* **62** (4), 375–383. https://doi.org/10.1097/MAT.0000000000000388 (Jul. 2016).
3. Mehra, M. R. et al. Apr., A Fully Magnetically Levitated Left Ventricular Assist Device - Final Report, *N. Engl. J. Med.*, vol. 380, no. 17, pp. 1618–1627, (2019). https://doi.org/10.1056/NEJMoa1900486
4. Malick, A. et al. Development of de Novo aortic insufficiency in patients with heartmate 3. *Ann. Thorac. Surg.* **114** (2), 450–456. https://doi.org/10.1016/j.athoracsur.2021.08.074 (Aug. 2022).
5. Romero Dorta, E. et al. Potential benefits of aortic valve opening in patients with left ventricular assist devices. *Artif. Organs*. https://doi.org/10.1111/aor.14891 (2024).
6. Ayre, P. J., Lovell, N. H. & Woodard, J. C. Non-invasive flow estimation in an implantable rotary blood pump: a study considering non-pulsatile and pulsatile flows, *Physiol. Meas.*, vol. 24, no. 1, pp. 179–189, Feb. (2003). https://doi.org/10.1088/0967-3334/24/1/313
7. Bertram, C. D. Measurement for implantable rotary blood pumps, *Physiol. Meas.*, vol. 26, no. 4, pp. R99–R117, Aug. (2005). https://doi.org/10.1088/0967-3334/26/4/R01
8. Naiyanetr, P. et al. Continuous assessment of cardiac function during rotary blood pump support: a contractility index derived from pump flow. *J. Heart Lung Transpl. Off Publ Int. Soc. Heart Transpl.* **29** (1), 37–44. https://doi.org/10.1016/j.healun.2009.05.032 (Jan. 2010).
9. Moscato, F., Granegger, M., Naiyanetr, P., Wieselthaler, G. & Schima, H. Evaluation of left ventricular relaxation in rotary blood pump recipients using the pump flow waveform: a simulation study. *Artif. Organs*. **36** (5), 470–478. https://doi.org/10.1111/j.1525-1594.2011.01392.x (May 2012).
10. Granegger, M., Schima, H., Zimpfer, D. & Moscato, F. Assessment of aortic valve opening during rotary blood pump support using pump signals. *Artif. Organs*. **38** (4), 290–297. https://doi.org/10.1111/aor.12167 (2014).
11. Granegger, M. et al. Continuous monitoring of aortic valve opening in rotary blood pump patients. *IEEE Trans. Biomed. Eng.* **63** (6), 1201–1207. https://doi.org/10.1109/TBME.2015.2489188 (Jun. 2016).
12. Hayward, C. et al. Pump speed waveform analysis to detect aortic valve opening in patients on ventricular assist device support. *Artif. Organs*. **39** (8), 704–709. https://doi.org/10.1111/aor.12570 (2015).
13. Clifford, R. et al. Beat-to-beat detection of aortic valve opening in heartware left ventricular assist device patients. *Artif. Organs*. **43** (5), 458–466. https://doi.org/10.1111/aor.13381 (2019).
14. Moscato, F., Granegger, M., Edelmayer, M., Zimpfer, D. & Schima, H. Continuous monitoring of cardiac rhythms in left ventricular assist device patients. *Artif. Organs*. **38** (3), 191–198. https://doi.org/10.1111/aor.12141 (2014).
15. Maw, M. et al. Development of Suction detection algorithms for a left ventricular assist device from patient data. *Biomed. Signal. Process. Control*. **69**, 102910. https://doi.org/10.1016/j.bspc.2021.102910 (Aug. 2021).
16. Belkin MN, Kagan V, Labuhn C, Pinney SP, Grinstein J. Physiology and clinical utility of heartmate pump parameters. *J. Card Fail.* **28** (5), 845–862. https://doi.org/10.1016/j.cardfail.2021.11.016 (May 2022).
17. Albert, C. L. & Estep, J. D. How to optimize patient selection and device performance of the newest generation left ventricular assist devices. *Curr. Treat. Options Cardiovasc. Med.* **21** (9), 48. https://doi.org/10.1007/s11936-019-0748-x (Aug. 2019).
18. Adamopoulos, S. et al. Right heart failure with left ventricular assist devices: Preoperative, perioperative and postoperative management strategies. A clinical consensus statement of the Heart Failure Association (HFA) of the ESC, *Eur. J. Heart Fail.*, vol. n/a, no. n/a. https://doi.org/10.1002/ejhf.3323
19. Schlöglhofer, T. et al. HeartMate 3 Snoopy: noninvasive cardiovascular diagnosis of patients with fully magnetically levitated blood pumps during echocardiographic speed ramp tests and Valsalva maneuvers. *J. Heart Lung Transpl.* **0** (0). https://doi.org/10.1016/j.healun.2023.09.011 (Sep. 2023).
20. Consolo, F., Pieri, M., Pazzanese, V., Scandroglio, A. M. & Pappalardo, F. Longitudinal analysis of pump parameters over long-term support with the HeartMate 3 left ventricular assist device, *J. Cardiovasc. Med. Hagerstown Md*, vol. 24, no. 10, pp. 771–775, Oct. (2023). https://doi.org/10.2459/JCM.0000000000001522
21. Uriel, N. et al. Development of a novel echocardiography ramp test for speed optimization and diagnosis of device thrombosis in Continuous-Flow left ventricular assist devices. *J. Am. Coll. Cardiol.* **60**, 1764–1775. https://doi.org/10.1016/j.jacc.2012.07.052 (Oct. 2012).
22. Bender, M. et al. An atraumatic mock loop for realistic hemocompatibility assessment of blood pumps. *IEEE Trans. Biomed. Eng.* 1–12. https://doi.org/10.1109/TBME.2023.3346206 (2023).
23. Colacino, F. M. et al. A modified elastance model to control mock ventricles in real-time: numerical and experimental validation, *ASAIO J. Am. Soc. Artif. Intern. Organs*, vol. 54, no. 6, pp. 563–573, 2008, vol. 54, no. 6, pp. 563–573, 2008, (1992). https://doi.org/10.1097/MAT.0b013e31818a5c93
24. Gupta, S. et al. Normalisation of haemodynamics in patients with end-stage heart failure with continuous-flow left ventricular assist device therapy. *Heart Lung Circ.* **23** (10), 963–969. https://doi.org/10.1016/j.hlc.2014.04.259 (Oct. 2014).
25. Errill, E. W. Rheology of blood. *Physiol. Rev.* **49** (4), 863–888. https://doi.org/10.1152/physrev.1969.49.4.863 (Oct. 1969).
26. Késmárky, G., Kenyeres, P., Rábai, M. & Tóth, K. Plasma viscosity: a forgotten variable. *Clin. Hemorheol Microcirc.* **39**, 1–4 (2008).
27. Uriel, N. et al. Impact of hemodynamic ramp Test-Guided HVAD speed and medication adjustments on clinical outcomes: the RAMP-IT-UP multicenter study. *Circ. Heart Fail.* **12** (4), e006067. https://doi.org/10.1161/CIRCHEARTFAILURE.119.006067 (Apr. 2019).
28. Bland, J. M. & Altman, D. G. STATISTICAL METHODS FOR ASSESSING AGREEMENT BETWEEN TWO METHODS OF CLINICAL MEASUREMENT, p. 9 .
29. Reyes, C. et al. Accuracy of the HVAD pump flow Estimation algorithm. *ASAIO J.* **62** (1), 15–19. https://doi.org/10.1097/MAT.0000000000000295 (Jan. 2016).
30. Stephens, A. F. et al. HeartWare HVAD Flow Estimator Accuracy for Left and Right Ventricular Support, *ASAIO J. Am. Soc. Artif. Intern. Organs*, vol. 67, no. 4, pp. 416–422, Apr. 2021, vol. 67, no. 4, pp. 416–422, Apr. 2021, (1992). https://doi.org/10.1097/MAT.0000000000001247
31. Granegger, M., Moscato, F., Casas, F., Wieselthaler, G. & Schima, H. Development of a pump flow estimator for rotary blood pumps to enhance monitoring of ventricular function. *Artif. Organs*. **36** (8), 691–699. https://doi.org/10.1111/j.1525-1594.2012.01503.x (2012).
32. Elenkov, M. et al. Estimation methods for viscosity, flow rate and pressure from Pump-Motor assembly parameters. *Sensors* **20** (5), 1451. https://doi.org/10.3390/s20051451 (Mar. 2020).
33. Shida, S., Masuzawa, T. & Osa, M. Effects of gravity on flow rate estimations of a centrifugal blood pump using the eccentric position of a levitated impeller, *Int. J. Artif. Organs*, vol. 43, no. 12, pp. 774–781, Dec. (2020). https://doi.org/10.1177/0391398820917149
34. Shida, S., Masuzawa, T. & Osa, M. Flow rate estimation of a centrifugal blood pump using the passively stabilized eccentric position of a magnetically levitated impeller, *Int. J. Artif. Organs*, vol. 42, no. 6, pp. 291–298, Jun. (2019). https://doi.org/10.1177/0391398819833372
35. Hijikata, W., Rao, J., Abe, S., Takatani, S. & Shinshi, T. Sensorless Viscosity Measurement in a Magnetically-Levitated Rotary Blood Pump, *Artif. Organs*, vol. 39, no. 7, pp. 559–568, Jul. (2015). https://doi.org/10.1111/aor.12440
36. Schmid, C. et al. Sep., First Clinical Experience With the Incor Left Ventricular Assist Device, *J. Heart Lung Transplant.*, vol. 24, no. 9, pp. 1188–1194, (2005). https://doi.org/10.1016/j.healun.2004.08.024
37. Hetzer, R. et al. First experiences with a novel magnetically suspended axial flow left ventricular assist device. *Eur. J. Cardiothorac. Surg.* **25** (6), 964–970. https://doi.org/10.1016/j.ejcts.2004.02.038 (Jun. 2004).

38. Hohmann, S. et al. Initial experience with telemonitoring in left ventricular assist device patients. *J. Thorac. Dis.* **1** (1). https://doi.org/10.21037/jtd.2018.10.37 (Apr. 2019).
39. Knüppel, F., Thomas, I., Wurm, F. H. & Torner, B. Suitability of Different Blood-Analogous Fluids in Determining the Pump Characteristics of a Ventricular Assist Device, *Fluids*, vol. 8, no. 5, Art. no. 5, May (2023). https://doi.org/10.3390/fluids8050151
40. Dobarro, D. et al. Impact of aortic valve closure on adverse events and outcomes with the heartware ventricular assist device. *J. Heart Lung Transpl.* **36** (1), 42–49. https://doi.org/10.1016/j.healun.2016.08.006 (2017).

Acknowledgements

We want to thank Thomas Schlöglhofer and his group of for their support in data extraction of the HM3 data. Furthermore, we thank the entire VAD team of the Medical University of Vienna, namely our cardiac surgeons, our cardiologists and especially our VAD Coordinator for their continuous support during this study. The financial support by the Austrian Federal Ministry of Labor and Economy, the National Foundation for Research, Technology and Development and the Christian Doppler Research Association is gratefully acknowledged.

Author contributions

T.A. wrote the original draft, performed data curation, processing, formal analysis, investigation, software development, and visualization. M.GRU. contributed to method development, data acquisition, and results generation, and wrote parts of the manuscript. P.A. supervised the work and contributed to manuscript writing and editing. M.R. established methods, supervised the work, and contributed to manuscript writing and editing. S.J. supervised the work and developed methods. D.Z. conceptualized the study, supervised the work, and reviewed and edited the manuscript. M.GRA. conceptualized the study, developed methodologies, worked on software and visualization, supervised the work, and reviewed and edited the manuscript. All authors reviewed and approved the final manuscript.

Declarations

Competing interests

The authors declare no competing interests.

Additional information

Supplementary Information The online version contains supplementary material available at https://doi.org/10.1038/s41598-025-03743-9.

Correspondence and requests for materials should be addressed to M.G.